Tellus (1999), 51B, 233–248
Printed in UK – all rights reserved

TELLUS
ISSN 0280–6495

Long-term variability in the global carbon cycle inferred from a high-precision CO_2 and $\delta^{13}C$ ice-core record

By C. M. TRUDINGER[1,2]*, I. G. ENTING[1,2], R. J. FRANCEY[1,2], D. M. ETHERIDGE[1] and P. J. RAYNER[1,2], [1]*CSIRO Atmospheric Research, PMB 1, Aspendale, Vic. 3195 Australia;* [2]*Cooperative Research Centre for Southern Hemisphere Meteorology, Monash University, Clayton, Vic. 3168, Australia*

(Manuscript received 14 January 1998; in final form 24 November 1998)

ABSTRACT

The new high precision Law Dome ice core record of CO_2 and $\delta^{13}CO_2$ is used with a 1-D global carbon cycle model to investigate natural variability in the carbon cycle and the anthropogenic CO_2 perturbation, focusing on variations on time-scales of centuries. A major feature of the ice core record is the decrease in CO_2, and increase in $\delta^{13}C$, through the "Little Ice Age" period (roughly 1550–1800). We show that this observed decrease in CO_2 is consistent with the effect of decreased temperature on either terrestrial or oceanic exchange, however the increase in $\delta^{13}C$ favors a terrestrial response to cooling. We perform single deconvolution model calculations which generally give good agreement with observed variations in CO_2, $\delta^{13}C$ and $\Delta^{14}C$ data for different reservoirs and due to both natural and anthropogenic causes. The fit to pre-bomb $\Delta^{14}C$ is improved by using an ice core ^{10}Be record to represent the natural production of ^{14}C due to cosmic rays, however the uncertainties in interpreting the ^{10}Be are as yet too large to use pre-bomb $\Delta^{14}C$ to better constrain the model parameters.

1. Introduction

Atmospheric CO_2 concentration has increased by more than 25% since pre-industrial times as a result of anthropogenic activities, and will continue to increase in the future. This is of considerable concern because of the effect CO_2 has on the earth's radiation budget. Carbon cycle models are used extensively to predict future levels of CO_2, but reliable predictions depend on being able to accurately model the carbon cycle in the present and past. It is important to keep in mind that the anthropogenic CO_2 perturbation sits on top of the natural variability of the carbon cycle. While such variation has commonly been treated as "noise" whose time-averaged effect is zero, much of our understanding of the carbon cycle is based on interpreting indirect information. Such inferences can be extremely sensitive to "noise", so we need to understand the magnitude and characteristics of natural variability.

Records of atmospheric CO_2 reconstructed from measurements of air trapped in polar ice provide an excellent way to study the carbon cycle over recent centuries. A number of different modelling approaches are possible: models are generally used to either calculate concentrations for a given source history (forward calculation) or to deduce the source history required to match specified concentrations (inverse calculation, or deconvolution). Deconvolution techniques are commonly applied to concentrations from ice core records, and the two types of calculation that have been used have become known as the single deconvolution and double deconvolution. In a single deconvolution, the source due to fossil fuel burning and uptake by the ocean are usually specified and

* Corresponding author.
E-mail: cathy.trudinger@dar.csiro.au

mass balance is used to determine an additional flux that is attributed to biospheric uptake or release (Siegenthaler and Oeschger, 1987; Siegenthaler and Joos, 1992; Bruno and Joos, 1997). These single deconvolutions rely on ocean models to determine oceanic CO_2 uptake. In general, simple ocean carbon cycle models mainly describe the "passive" response of the ocean to changing atmospheric levels, and are not able to capture some of the variation in ocean uptake, for example on ENSO time-scales. More complex, mechanistic models are required to model the "active" response induced by climate variations. Measurements of the CO_2 isotopes, ^{13}C and ^{14}C, are often used in the single deconvolution to either calibrate the model components, or check the overall calculation. In a double deconvolution, the fossil-fuel source is again specified, and the stable isotope, ^{13}C, is used with CO_2 to partition the deduced source/sink into oceanic and terrestrial components (Keeling et al., 1989; Joos and Bruno, 1998). The method is the same as that used by Francey et al. (1995), with CO_2 and ^{13}C budget equations from Tans et al. (1993), but with models being used to calculate the isotopic disequilibrium terms.

A new high quality ice core record of $\delta^{13}CO_2$, from Law Dome, Antarctica (Francey et al., 1999) adds substantially to the data available for use in these modelling studies. The Law Dome CO_2 record (Etheridge et al., 1996) and $\delta^{13}C$ record are shown in Fig. 1. The record, which extends back almost 1000 years, is made up of measurements from 3 ice cores (DE08, DE08-2 and DSS) on Law Dome, East Antarctica, as well as measurements of air collected from the firn at DE08-2. The record has very high time-resolution due to the high accumulation rates at these sites. In addition, the high accumulation rate means that very recent air is trapped in the ice, such that the ice core record overlaps with direct atmospheric measurements for a number of tracers. This, along with the firn measurements, allows us to link ice core measurements and recent direct atmospheric records.

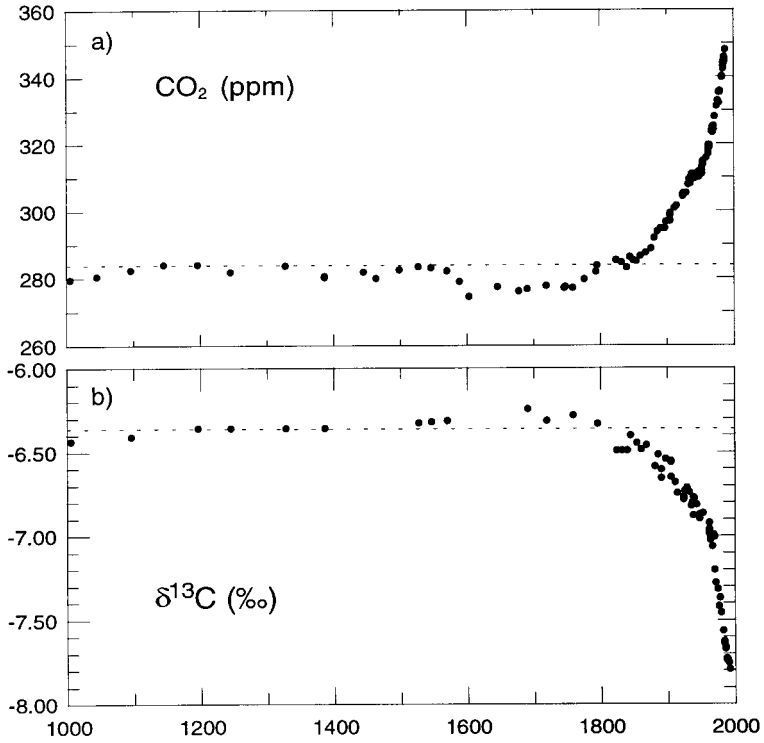

Fig. 1. (a) Law Dome ice core CO_2 record from Etheridge et al. (1996) and (b) $\delta^{13}C$ record from Francey et al. (1999).

The change in $\delta^{13}C$ from pre-industrial times to the present provides a useful constraint for carbon cycle studies, and many modellers have used the Siple $\delta^{13}C$ ice core record (Friedli et al., 1986) as a check on their results (Siegenthaler and Joos, 1992; Jain et al., 1996; Lassey et al., 1996). The Law Dome $\delta^{13}C$ record greatly improves the precision of the measured change in $\delta^{13}C$, which means that it can be used as a much stronger constraint. In comparison with the Siple record, the Law Dome $\delta^{13}C$ record is considerably less scattered, and has been corrected for the effects of isotopic fractionation due to diffusion in the firn. The Siple ice core record ends in 1953, and levels have often been compared with modern measurements at a different site to determine the change in $\delta^{13}C$ since pre-industrial times, whereas firn measurements extend the Law Dome record up to 1993.

The pre-industrial CO_2 and $\delta^{13}C$ exhibit significant structure, so that it can not necessarily be assumed that the pre-industrial carbon cycle was in equilibrium. The Law Dome record shows that the level of CO_2 dropped by about 6 ppm around 1550, and stayed low until about 1800. At this time, $\delta^{13}C$ was the highest it has been since 1000. This period is around the time of reported low temperatures in Europe often referred to as the "Little Ice Age", (Grove, 1988). The Siple CO_2 and $\delta^{13}C$ ice core record began in 1744, and this has commonly been used as a starting point for modelling studies. As suggested by Enting (1992), the CO_2 increase between 1750 and 1800 was probably due to a recovery from the "Little Ice Age", and not the beginning of the industrial perturbation.

^{14}C is often used to calibrate models that predict the uptake of anthropogenic carbon. $\Delta^{14}C$ in the atmosphere varies both naturally and as a result of anthropogenic activities. In the 1950s and 1960s, bomb tests increased the amount of ^{14}C in the atmosphere to almost double the natural level. After test-ban treaties were set in place, atmospheric levels decreased as ^{14}C was taken up by the oceans and terrestrial biosphere. Bomb ^{14}C is very useful for calibrating models, however the time histories of bomb ^{14}C and anthropogenic CO_2 in the atmosphere are quite different — the input of bomb ^{14}C is dominated by a pulse in the early 1960s whereas CO_2 emissions have been approximately exponential. Questions have been raised about whether bomb ^{14}C is a good analogue for anthropogenic CO_2 due to the different forcing functions involved (Heimann and Maier-Reimer, 1996). $\Delta^{14}C$ also varies due to the input of ^{14}C-free fossil fuel CO_2, which reduces the atmospheric $\Delta^{14}C$; this is known as the Suess effect (Suess, 1955). Tree-ring $\Delta^{14}C$ measurements show a decrease of about 20‰ from 1900 to 1950 (after this, bomb ^{14}C overwhelms the Suess effect signal). However, the measured decrease is not due only to the Suess effect. The natural production of ^{14}C due to the interaction of cosmic rays with the atmosphere has significant variability. The production rate is believed to have decreased between 1900 and 1950, and this is thought to have been responsible for part of the measured $\Delta^{14}C$ decrease (Stuiver and Quay, 1981).

The change in ^{14}C due to variations in the natural production rate is needed to properly model the observed $\Delta^{14}C$ decrease in the first half of this century. Beer et al. (1988) showed a good correlation between variations of ^{14}C and ^{10}Be, another cosmogenic isotope, on time-scales of about 200 years, giving good evidence that their variations have a common cause (i.e., changes in their production rates due to changes in the cosmic ray flux). A number of studies have used variations in ^{14}C production rates determined from ice core ^{10}Be data in a carbon cycle model, and compared modelled and measured $\Delta^{14}C$ (Beer et al., 1994; Bard et al., 1997).

In this paper, we use a 1-D global carbon cycle model to look at variations in CO_2 and ^{13}C in the Law Dome firn and ice core record, and ^{14}C from tree-rings. In particular, we focus on modelling the anthropogenic perturbation, as well as natural variability on time-scales of centuries. We investigate three aspects of natural variability. Firstly we consider variations in the natural ^{14}C production rate. This does not affect the carbon cycle but does influence ^{14}C data that are used to interpret the carbon cycle. We also consider the carbon cycle variations associated with the Little Ice Age, within which time many carbon cycle models have been initiated from a pre-industrial equilibrium. Finally we consider the shorter-term temperature variations through the 20th century. The outline of the paper is as follows. In Section 2 we briefly describe the model, calibration of the model parameters and the data used. The single deconvolution calculation used in calibration of the model

parameters is discussed in detail in Section 3. Forward model calculations that investigate the possible role of temperature in causing the observed variations during the "Little Ice Age" are described in Section 4. We summarise the main conclusions in Section 5.

2. Model and data

We use a box-diffusion carbon cycle model (Enting and Lassey, 1993; Lassey et al., 1996) which has 2 well-mixed atmospheric reservoirs (troposphere and stratosphere), a 2-box biosphere (short- and long-lived), a surface ocean layer and an Oeschger et al. (1975) diffusive deep ocean. We model CO_2 and the isotopes ^{13}C and ^{14}C.

The model includes a source of CO_2 to the atmosphere from fossil fuel burning. The forward calculations described in Section 4 have a flux from the long-lived biosphere to the atmosphere due to land-use change, and enhancement of net primary production (NPP) due to CO_2 fertilisation. For the fertilisation we use the hyperbolic form given by Allen et al. (1987), where NPP at CO_2 concentration C is enhanced by factor

$$G(C) = G_\infty \frac{C - C_c}{C + b}, \tag{1}$$

where $G_\infty = 2.4$ is the limiting growth factor, $C_c = 80$ ppm is the compensation concentration below which photosynthesis ceases and

$$b = (G_\infty - 1)C_0 - G_\infty C_c$$

ensures that $G(C_0) = 1$ at the initial concentration C_0.

A number of our calculations incorporate the effect of changes in temperature on exchange between reservoirs. We model the response of the biospheric fluxes to changing temperature using Q_{10} relationships, i.e.,

$$F(T + \Delta T) = F(T) \times Q_{10}^{\Delta T/10}, \tag{2}$$

where $F(T)$ is the flux at temperature, T, and $Q_{10} = 2.0$ for soil respiration and 1.4 for NPP. These are typical Q_{10} values, and were used by Harvey (1989) in a number of globally aggregated terrestrial biosphere models. Defining global Q_{10} values is difficult. For the calculations presented here, what matters more than the actual Q_{10} values is the fact that, globally speaking, respiration is more sensitive to temperature than NPP, which is what is expected (J. Lloyd, personal communication). This can be verified for particular ecosystems. For example, Grace et al. (1996) show that for a tropical rainforest, respiration is far more sensitive to temperature than is photosynthesis. In general, photosynthesis is less sensitive to temperature than respiration, especially at lower CO_2 concentrations. As NPP is the balance between plant respiration and photosynthesis, the Q_{10} value for NPP lies between the values of Q_{10} for plant respiration and photosynthesis, so is less than the respiration value. We can be reasonably confident of the sense of the change in CO_2 and the isotopes, however the magnitude of the change will be difficult to determine correctly with a globally aggregated biospheric model such as the one used here.

The model has two types of detrital flux in the ocean, organic and carbonate, which each have different penetration depths and isotopic fractionation relative to the inorganic carbon in the surface water (Enting and Lassey, 1993). The rate of remineralisation of the organic component decreases with depth following a power law given by Martin et al. (1987), while the carbonate component dissolves equally at all depths. The P_{CO_2} of the mixed layer is given by

$$P = P_0[1 + y\xi(y)], \tag{3}$$

where $P_0 = 284$ is a reference partial pressure (set to the pre-industrial CO_2 concentration in the atmosphere), $y = (q - q_0)/q_0$, q is the dissolved inorganic carbon concentration, with $q_0 = 2.089$ mol m^{-3} and the buffer factor, ξ, is given by

$$\xi(y) = 9.36 + 59.56y + 4558y^3,$$

from Bacastow (1981). We use the same temperature-dependence of the buffer factor, ξ, as Enting and Pearman (1982). This has the ocean partial pressure of CO_2 varying with temperature according to

$$P(T) \propto \frac{1 + 0.0389T + 0.000448T^2}{1780 - 20T}, \tag{4}$$

where T is in °C. Broecker (1974) give P as inversely proportional to K, the equilibrium constant for the reaction

$$H_2O + CO_2 + CO_3^- \rightleftharpoons 2HCO_3^- \tag{5}$$

and also inversely proportional to the solubility,

α. Temperature dependence of K is determined using data from Broecker and Peng (1974)

$$K = 1780 - 20T, \tag{6}$$

and α has temperature-dependence

$$\frac{\alpha_0}{\alpha} \simeq 1 + 0.0389T + 0.000448T^2 \tag{7}$$

determined using tabulated data from Hodgeman (1958), where α_0 is the solubility at 0°C.

For temperature-dependence of isotopic fractionation of air–sea exchange we follow Heimann and Keeling (1989) in using

$$\alpha_{ma} = \alpha_{am}\left(1.02389 - \frac{9.483}{T + 273.15}\right), \tag{8}$$

which equates the temperature-dependence of the kinetic fractionation factor for sea–air flux, α_{ma} with the equilibrium fractionation of gaseous CO_2 with respect to dissolved HCO_3^- measured by Mook et al. (1974), and assumes α_{am} (kinetic fractionation factor for air–sea flux) is constant. This gives very similar results to the temperature-dependence given by Zhang et al. (1995) for total DIC. (We have assumed that variations in isotopic fractionation of biospheric exchange are negligible.) The model uses temperature anomalies as deviations from 17°C for the ocean fluxes, as 17°C was suggested by T. Hirst (CSIRO, personal communication, 1995) as a reasonable estimate of the pre-industrial global average sea-surface temperature.

^{14}C from bomb detonation and natural production due to cosmic rays are both put into the model stratosphere. The time variation of the natural ^{14}C production is determined from a record of ^{10}Be using

$$^{14}C \text{ prod} = A + B(^{10}Be(t) - C), \tag{9}$$

where A is the mean global ^{14}C production rate, C is a mean ^{10}Be concentration and B scales variations in ^{10}Be concentration to ^{14}C production. A, B and C are all tuned in the model's overall calibration procedure. We tune the mean ^{10}Be concentration, C, rather than just using the mean for the particular record because the record mean may not be the same as the long-term mean, around which we are assuming variations are proportional to variations in global ^{14}C production rate.

The model parameters are calibrated using a Bayesian calibration technique, which is described by Enting and Lassey (1993), and also by Enting and Pearman (1987) for a slightly different model configuration. Briefly, the calibration procedure tunes the model parameters to minimise the sum of squares of differences between model results and observations, as well as the sum of squares of deviations of the parameters from independent prior estimates of the parameters. The prior estimates of the parameters are included to stabilise the calibration, and to make use of the fact that we already know the range of reasonable values for most of the parameters. An important advantage of the Bayesian calibration technique is that many of the model parameters can be tuned simultaneously, and to a number of very different types of data, rather than having to tune the different components of the model separately.

We calibrate the model using single deconvolution calculations, where we specify the fluxes due to fossil fuel burning and land-use change, and calculate the net terrestrial exchange required for the modelled CO_2 to follow a spline fit through the Law Dome CO_2 record. Ocean uptake is calculated by the model. The CO_2 spline fit (Fig. 2a) is a weighted spline, where different ice core measurements are given different weights to vary the smoothing throughout the record. Before 1832, when there is only DSS data, the smoothing varies with data density. After 1832, DE08 and DE08-2 are weighted higher than DSS to take into account the higher time resolution of DE08 due to the higher accumulation rate at the site. The spline has 50% attenuation for periods of about 20 years for the DE08 and DE08-2 measurements, while the smoothing varies for DSS.

Data used to calibrate the model are the following: 75 tree-ring $\Delta^{14}C$ measurements between 1200–1945 from Stuiver and Becker (1993), needed primarily to tune the parameters that use ^{10}Be to reconstruct ^{14}C production rate variations (data are detrended, as will be explained in Section 3); 2 ocean-surface $\Delta^{14}C$ values, (−59‰ in 1958 and 110‰ in 1973) based on Broecker et al. (1960) and GEOSECS (Broecker et al., 1985); 2 bomb ^{14}C ocean inventories (difference of 1974 and 1975 from 1955 giving 299 and 311×10^{26} atoms, respectively) from Duffy and Caldeira (1995), based on GEOSECS, but adjusted to be global values using a 3-D ocean model; 6 tropospheric $\Delta^{14}C$ values, 1967–1987; 4 stratospheric ^{14}C

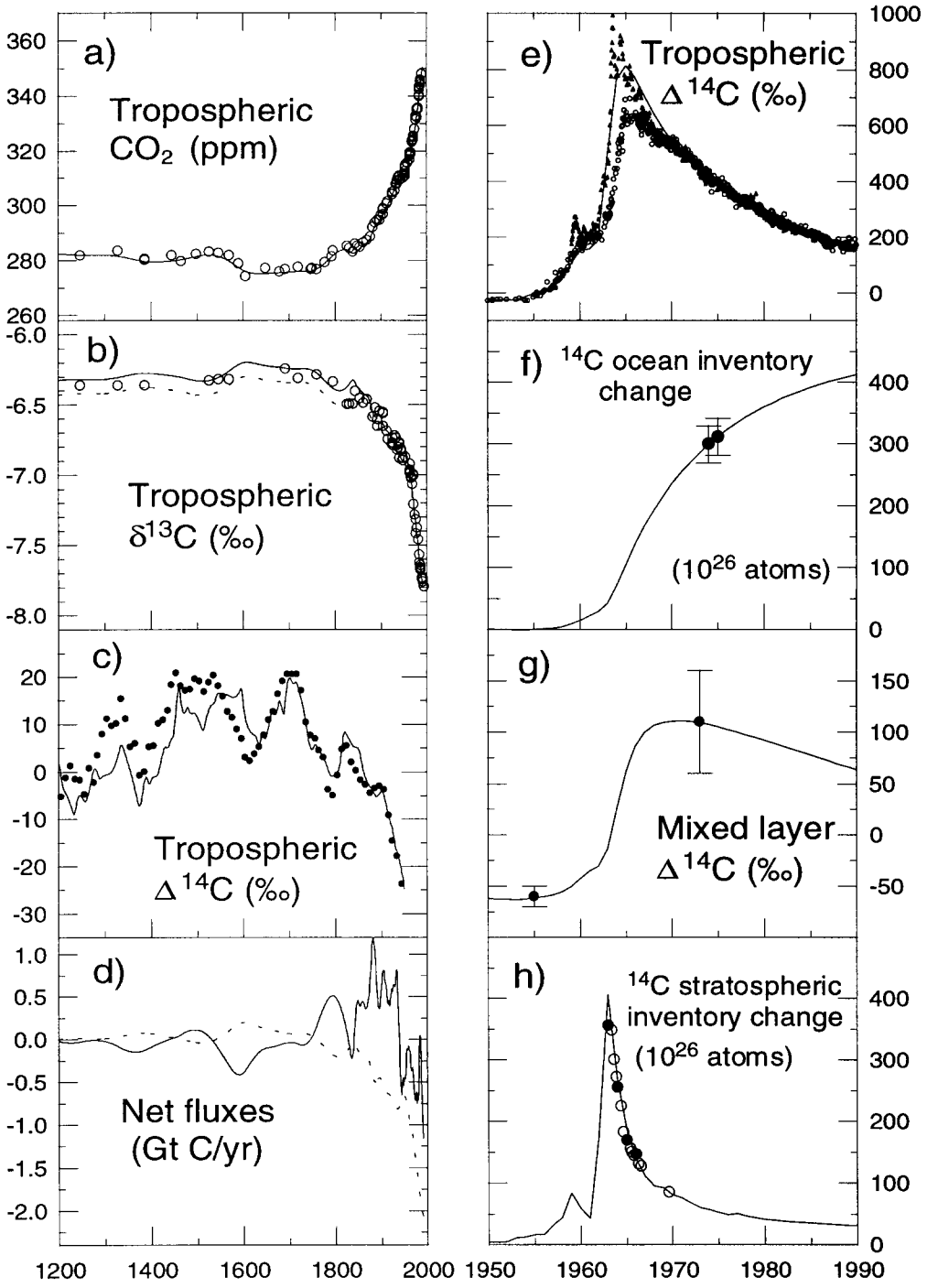
a)
Tropospheric
CO_2 (ppm)
b)
Tropospheric
$\delta^{13}C$ (‰)
c)
Tropospheric
$\Delta^{14}C$ (‰)
d)
Net fluxes
(Gt C/yr)
e)
Tropospheric
$\Delta^{14}C$ (‰)
f)
^{14}C ocean inventory
change
(10^{26} atoms)
g)
Mixed layer
$\Delta^{14}C$ (‰)
h)
^{14}C stratospheric
inventory change
(10^{26} atoms)
1200
1400
1600
1800
2000
1950
1960
1970
1980
1990

Fig. 2.

inventories from Tans (1981), which are based on measurements by Telegadas (1971); 1 $\Delta^{14}C$ deep ocean value (-150‰ in 1973) from GEOSECS; 1 deep ocean ΣCO_2 (2.34 in 1973) from GEOSECS. Apart from the deep ocean ΣCO_2 observation, the calibration data is all ^{14}C data. $\delta^{13}C$ data are not used for calibration, but the model calculates $\delta^{13}C$, which is compared with the Law Dome $\delta^{13}C$ ice core record. ^{13}C therefore acts as an important independent check on the model.

Our model calculations start with an initial state in equilibrium. We try to minimise the possible problems associated with making this steady state assumption by beginning our calculations at a flat part of the ice core record. The earliest relatively steady period in the Law Dome CO_2 record is around 1200, and we start our calculations then, assuming that at that time the carbon cycle was close to equilibrium. The horizontal lines in Figs. 1a,b indicate the 1200 CO_2 and $\delta^{13}C$ levels.

We use estimates of the source due to fossil fuel burning from Keeling (1997) between 1860 and 1949, with a linear increase from zero between 1840 and 1860, and from Marland and Boden (1997) after 1950. The $\delta^{13}C$ of the fossil-fuel source is taken from Andres et al. (1998). Land-use change estimates are from Houghton (1995). Since the net biotic flux, $B(t)$, in the model is a sum of forcing, $D(t)$, and a relaxation to equilibrium, Houghton's estimates of $B(t)$ need to be converted to $D(t)$ by using

$$D(t) = B(t) + \lambda_L \int_{1700}^{t} B(t')\,dt', \tag{10}$$

where λ_L is the inverse turnover time of the long-lived biosphere. The quantity $D(t)$ has no real significance in terms of land-use change fluxes, but is a model-dependent quantity needed in forward calculations to ensure that the net flux due to land-use change matches the given estimates. It is required because the long-lived biospheric reservoir includes both undisturbed and disturbed systems so its size is not fixed. This is described further in Enting and Lassey (1993).

The bomb detonation history of Enting (1982) is used, and the amount of ^{14}C per megaton TNT yield is tuned in the model's calibration procedure. The ^{10}Be ice core record from South Pole (Raisbeck et al., 1990) is used for calculating the natural production of ^{14}C due to cosmic rays. It turns out that the tuned mean ^{10}Be (i.e., variable C in eq. (9)) is very close to the mean for the record (382×10^2 atoms g^{-1}).

Table 1 lists the model parameters. Prior estimates and uncertainties are given for those parameters which were tuned in the present calibration procedure. The biospheric reservoir sizes and fluxes have been chosen to give the same isotopic pulse response as the biospheric model of Emanuel et al. (1981). Other parameters and many of the prior estimates use values from Enting and Lassey (1993), which were used in the IPCC calculations (Enting et al., 1994). The atmospheric turnover time and ocean diffusivity values are comparable to other estimates. The stratospheric turnover time is short compared to other estimates of around 3 years (we will discuss this briefly in Section 3), and the detrital fluxes are perhaps on the low end of current estimates.

3. Single deconvolution calculation

In this Section we discuss the single deconvolution calculation that was used in calibrating the model parameters. We look at the fit to the $\delta^{13}C$ and ^{14}C data and the calculated CO_2 net fluxes. The model has been calibrated using the data described in Section 2 (all ^{14}C data except for one ocean ΣCO_2 observation). Figs. 2b–2h show model output compared to a number of different observations, only some of which have been used

Fig. 2. (a) Spline fit to CO_2 record. (b) Law Dome $\delta^{13}C$ record and modelled $\delta^{13}C$ from single deconvolution calculation, with CO_2 tracking spline fit (solid line). The dashed line shows $\delta^{13}C$ calculated with the ocean response to the temperature increase this century. (c) Calculated young biospheric $\Delta^{14}C$, with observations from Stuiver and Becker (1993). (d) Net biospheric (solid line) and oceanic (dashed line) flux deduced in the single deconvolution. (e) Tropospheric $\Delta^{14}C$. Observations are from New Zealand (Manning and Melhuish, 1994) (circles) and Vermunt, Austria (Levin et al., 1985) (triangles). (f) Bomb ^{14}C ocean inventory, with data from Duffy and Caldeira (1995). (g) Mixed layer $\Delta^{14}C$. (h) Stratospheric ^{14}C inventory, with data from Tans (1981).

Table 1. *Model parameters obtained by fitting ^{14}C data and deep ocean carbon content in a single deconvolution; prior estimates and (prior) uncertainties are given for the parameters tuned in the calibration procedure*

Parameter	Value	Prior	Uncert.
ocean surface layer depth (m)	75		
ocean depth (m)	3800		
ocean surface area (10^{12} m)	361.16		
tropospheric : stratospheric mass ratio	80 : 20		
ppm per Gt in the atmosphere	0.47		
deep ocean diffusivity ($m^2\ y^{-1}$)	5524	5364	2000
atmospheric C turnover w.r.t. ocean (y)	8.76	12	2
stratospheric C turnover time (y)	1.8	4.0	1.0
net primary productivity (GtC y^{-1})	84.3		
turnover time of young biosphere to atmosphere (y)	6.3		
turnover time of young biosphere to old biosphere (y)	20.3		
turnover time of old biosphere (y)	54.5		
size of young biosphere (Gt)	405.3		
size of old biosphere (Gt)	1089		
bomb ^{14}C production (10^{26} atoms per Mt TNT yield)	3.07	2.75	3.0
A = mean ^{14}C production due to cosmic rays (10^{26} atoms y^{-1})	2.56	2.5	1.5
B = factor relating ^{10}Be variations to ^{14}C production variations ($10^{-3} \times (10^{26}$ atom $^{14}C\ y^{-1})/(10^2$ atoms $g^{-1})$)	5.085	4.0	12.0
C = mean ^{10}Be concentration (10^2 atoms g^{-1})	384	382	7
detrital parameters			
carbonate flux (Gt y^{-1})	2.37	4.0	3.0
organic flux (Gt y^{-1})	3.28	4.0	3.0
carbonate isotopic fractionation (‰)	0		
organic isotopic fractionation (‰)	−24		
isotope fractionation factors ($^{13}C/^{12}C$)			
atmosphere–ocean	0.9975		
ocean–atmosphere	0.9892		
atmosphere–biosphere	0.982		
biosphere–atmosphere	1		

to calibrate the model. In general, the filled symbols indicate data used for calibration.

3.1. $\delta^{13}C$

The calculated $\delta^{13}C$ is shown by the solid line in Fig. 2b. The initial $\delta^{13}C$ level (in this case at 1200 AD) has been adjusted to ensure that the 1990 $\delta^{13}C$ matches observations. The model captures well the overall decrease in $\delta^{13}C$ and some of the decadal features. The modelled 1200–modern difference agrees with the observations to within the uncertainty of 0.05‰ estimated for this quantity by Francey et al. (1999).

This calculation doesn't include any effects of variation in temperature. The dashed line in Fig. 2b shows the $\delta^{13}C$ calculated by including the effect on ocean exchange of the increase in temperature of about 0.5°C that has been measured over this century. For this calculation, the record of observed global temperature from Jones and Briffa (1992) is used. The modelled $\delta^{13}C$ pre-industrial–modern difference is reduced by about 0.1‰ compared to the constant temperature case, but is still very close to the observations. This case is not shown in any of the other parts of Fig. 2 because the difference between the two cases is negligible for ^{14}C and the net fluxes. (We only include temperature-dependence for the ocean and not the biosphere because the model already calculates biospheric exchange by requiring that modelled CO_2 follow observations, so temperature-dependence of NPP and soil respiration essentially makes no difference to the net fluxes or the calculated $\delta^{13}C$.)

In this single deconvolution calculation, the net

fluxes are determined from the CO_2 and the ocean model, and $\delta^{13}C$ is calculated as a "by-product". The fact that the modelled $\delta^{13}C$ agrees well with the observations is a valuable independent check on the model. The effect of the increase in temperature doesn't have a dramatic effect on the $\delta^{13}C$. Joos and Bruno (1998) in their double deconvolution calculation, calculate the sensitivity to the change in isotopic fractionation due to temperature and find that it makes only a small difference to the calculated net fluxes on a decadal timescale, always less than 0.2 GtC y^{-1}. There are a number of other things that could alter the match with the $\delta^{13}C$ that we haven't included here. For example, a change in the ratio of C3 to C4 plants over time due to land-use change may have changed the globally averaged isotopic discrimination of the biosphere, which will alter the change in $\delta^{13}C$. Also, the CO_2 and $\delta^{13}C$ change measured in the Law Dome record actually applies for the high latitudes of the southern hemisphere, while the model considers global levels. The addition of fossil fuel CO_2 mainly in the northern hemisphere has caused the spatial distribution of CO_2 and $\delta^{13}C$ in the atmosphere to change over time, and therefore altered the difference between high southern latitudes and the global mean. The effect of ignoring the difference between Law Dome and global levels for $\delta^{13}C$ is partly compensated for by doing the same for CO_2. If treated we expect it would give a slightly greater $\delta^{13}C$ decrease, but probably within the current uncertainty on the measurements.

The change in $\delta^{13}C$ from pre-industrial levels to the present provides useful information for modelling the integrated uptake of anthropogenic CO_2. In a double deconvolution, the change in $\delta^{13}C$ is used with the CO_2 to partition the oceanic and biospheric fluxes. The $\delta^{13}C$ change therefore becomes quite important. It is worth noting that $\delta^{13}C$ can provide a stronger constraint on the integrated uptake of CO_2 than on net fluxes. Deconvolution calculations such as this one, or the double deconvolution of Joos and Bruno (1998), begin at pre-industrial levels and estimate fluxes up to some recent time. This gives them an advantage over studies that only cover a short period in recent decades (Enting et al., 1995; Francey et al., 1995; Rayner et al., 1999) because starting at pre-industrial levels allows the disequilibrium flux terms in the ^{13}C budget (i.e., the product of gross fluxes and isotopic disequilibria for the biosphere and ocean) to be determined as part of the calculation. Fortunately, assumptions about model structure don't strongly affect the calculated disequilibrium fluxes, and therefore the net fluxes. We tested the sensitivity of the calculated disequilibrium fluxes to model structure for a 5 box biosphere model from Emanuel (1981) and found that large variations in the overturning times of the reservoirs produced only quite small changes in the calculated disequilibrium fluxes. This is because of compensations between the gross fluxes and isotopic disequilibria, meaning that their product is reasonably stable. This happens because the model calculates both of these quantities, ensuring consistency of fluxes and disequilibria with the whole past history. Studies that don't do this cannot reliably use just CO_2 and $\delta^{13}C$ to partition net fluxes, so require additional information such as O_2 changes (Rayner et al., 1999), or use disequilibrium fluxes from independent models.

The global disequilibrium flux is very difficult to estimate from direct measurements. Our model calculation gives global values averaged over the period 1980–89 of 55.4 GtC ‰ y^{-1} for the ocean and 22.2 GtC ‰ y^{-1} for the biosphere, giving a total of 77.6 GtC ‰ y^{-1}. Joos and Bruno (1998) give a comparison of disequilibrium values from a number of studies. The values (in GtC ‰ y^{-1}) from their double deconvolution for 1987 are 50.4 and 26.4 for the ocean and biosphere, respectively, with a total of 76.8. Our 1987 values are 58.1 and 22.9, totaling 81.0. R. L. Langenfelds (CSIRO, personal communication, 1998) determines the total global isotopic disequilibrium flux for 1980–89 to be 88 ± 20 GtC ‰ y^{-1} by using the trend in atmospheric O_2 to partition CO_2 uptake, then comparing with the ^{13}C budget. Rayner et al. (1999) predict a disequilibrium flux of 79 GtC ‰ y^{-1} for 1980–89 using the same O_2 data in their space–time synthesis inversion. The two O_2 results differ slightly because of different assumptions and methods used in the calculations, but they are both close to the values obtained by tracking the ice core records, which is a very encouraging result.

3.2. ^{14}C production from ^{10}Be data

Fig. 2c shows tree-ring measurements from Stuiver and Becker (1993) with modelled $\Delta^{14}C$.

The South Pole ^{10}Be record from Raisbeck et al. (1990) is used to determine variations in ^{14}C production rate. Variations in the production rates of both ^{10}Be and ^{14}C are related to changes in cosmic ray flux, and are therefore very similar, but the geochemical behaviour of the two isotopes in the atmosphere is quite different. ^{14}C is oxidised to $^{14}CO_2$, which is quite well mixed in the atmosphere, and becomes involved in exchanges between reservoirs. ^{10}Be attaches to aerosols, and is removed from the atmosphere after a mean residence time of no longer than 1 to 2 years (Beer et al., 1994). This means that ^{10}Be can have significant spatial variability. According to Bard et al. (1997), ^{10}Be measured in Antarctic ice is mainly produced at high latitudes. Solar modulation is higher at high latitudes than at the equator due to the orientation of the magnetic field, so the relative amplitude of ^{10}Be variations around the mean in polar ice cores probably overestimates variation in global production. Bard et al. use a "Polar Enhancement Coefficient" (PEC) of about 0.6 to take account of this effect. Our parameter B in eq. (9) includes this effect in its conversion from ^{10}Be concentration to global ^{14}C production rate. The tree-ring data in Fig. 2c are detrended for the long-term increase due to the change in the earth's geomagnetic field intensity by subtracting the sinusoidal function derived by Houtermans (1971) and given in Stuiver and Quay (1980). South Pole ^{10}Be reflects mainly polar production, which should not be affected much by variations in the geomagnetic field. Bard et al. (1997) also detrended the ^{14}C data for comparison with model results.

Our main reason for reconstructing ^{14}C production rate variations from ^{10}Be was so that the ^{14}C Suess trend could be used as a constraint for calibrating the model parameters. The use of the ^{10}Be derived ^{14}C production rate compared to a constant production rate does give a much better fit to the observed Δ^{14}C. However, current uncertainties in the use of a single record of ^{10}Be to reconstruct ^{14}C production rates (i.e., spatial variability of ^{10}Be and the need for a PEC), mean that fitting the Suess trend doesn't presently help constrain the model parameters such as the turnover times of the reservoirs. A composite record with ^{10}Be from different sites, perhaps combined with other measures of cosmic ray variations would give better estimates of the ^{14}C production rate, so that pre-bomb ^{14}C could be used more confidently for carbon cycle model calibration.

3.3. *Bomb ^{14}C*

Figs. 2e–2h show modelled ^{14}C during and after the bomb tests. There is generally good agreement with observations, although the tropospheric Δ^{14}C around 1965 is perhaps 100‰ too high, with modelled global levels looking almost like the northern hemisphere measurements. The bomb ^{14}C ocean inventory estimates are from Duffy and Caldeira (1995). The stratospheric data shown in Fig. 2h is from Tans (1981), summarising measurements made by Telegadas (1971). The accuracy of these inventory estimates is questionable because the atmosphere would have been very inhomogeneous in the years soon after the bomb tests.

Hesshaimer et al. (1994) found a discrepancy in the budget of bomb ^{14}C when they compared model estimates of biospheric ^{14}C uptake and the change in ocean inventory of bomb ^{14}C (based on observations) with the observed change in the atmosphere. To balance the budget they required either 25% less ocean uptake of ^{14}C than that suggested by GEOSECS data, or 80% less biospheric uptake than that suggested by biosphere models. Joos (1994) compared the change in ^{14}C inventory from 1965 to 1989 for a number of models, and estimated a budget imbalance of $82 \pm 78 \times 10^{26}$ atoms when comparing the mean of the model estimates with observed atmospheric changes. Jain et al. (1997) claim that there is no discrepancy, given the large uncertainties involved, particularly in the stratospheric inventory, production rates of bomb ^{14}C and pre-bomb ocean Δ^{14}C values. Joos and Bruno (1998) suggested that estimates of the bomb test production and/or the stratospheric decrease are not compatible with ^{13}C and ^{14}C data.

The bomb ^{14}C budget has not been a particular focus of our study, however as we calibrate the model using mainly bomb ^{14}C, it is of some relevance. Our calculated changes in oceanic and biospheric ^{14}C inventory from 1965–89 are 304 and 70×10^{26} atoms, respectively, and very close to the model averages given by Joos (1994). The model gives changes in tropospheric and stratospheric ^{14}C from 1965–89 of 181 and 155×10^{26} atoms, respectively, both of which are higher than the observed changes quoted by Joos (1994) as

150 and 100. We therefore do see an imbalance in the budget similar to Hesshaimer et al. (1994), however Figs. 2e,h show that our fit to the available observations is reasonable, given the large uncertainties involved. If we calibrate the model without trying to match the stratospheric measurements, as was done by Lassey et al. (1996), then we can get good agreement with all of the other measurements. The stratospheric turnover time chosen by the calibration procedure is quite fast. It seems likely that the calibration is giving us turnover of the lower stratosphere rather than total stratosphere in order to match the stratospheric observations. This would mean we are putting too much bomb ^{14}C into the model, which may explain why the bomb ^{14}C production parameter is higher than its prior estimate. Clearly the bomb ^{14}C budget needs more work to understand it properly, but this is probably better done with a more complex model of the atmosphere than this simple 2-box model.

3.4. *Calculated net fluxes*

The solid and dashed lines in Fig. 2d show the net biospheric and oceanic fluxes, respectively. These are similar to fluxes calculated by Bruno and Joos (1997) who also performed a single deconvolution with the Law Dome CO_2 record. The calculated biospheric flux shows higher frequency variation after about 1800 compared with before. This is seen because the ice core record resolves more of the CO_2 variation after 1800, and the biospheric flux is calculated by tracking the spline fit to these measurements. The oceanic flux before 1800 appears to be anticorrelated with the biospheric flux but with a lag. This lagged anticorrelation is probably an artifact of the modelling, occurring because in the model the biospheric flux is calculated from the time derivative of the CO_2 concentration, while the oceanic flux responds to the CO_2 level as well as the derivative. A double deconvolution, or more complex ocean model, should give more realistic partitioning of CO_2 fluxes.

4. Little ice age calculations

A particularly striking feature in the Law Dome CO_2 record is the low CO_2 level between about 1550 and 1800. This coincides with the period often referred to as the "Little Ice Age" (LIA), when there were reports of low temperatures and glacier advances in Europe (Grove, 1988). As discussed by Etheridge et al. (1996), the decrease in CO_2 is unlikely to have been the primary cause of the LIA cooling. It is more likely that the reduced temperature (driven by other factors) affected the carbon exchange between different reservoirs, changing the global CO_2 concentration level. $\delta^{13}C$ over this period is higher than the mean pre-industrial level, and we explore this fact as a means of determining the most likely processes involved.

In particular, we investigate the possible role of temperature in causing these changes in CO_2 and $\delta^{13}C$, by modelling separately the response of oceanic and terrestrial exchange to a decrease in temperature. We consider a hypothetical temperature record that decreases linearly between 1550–1600 then stays constant until 1750, when it increases linearly to its initial level in 1800 (Fig. 3a). The magnitude and timing of the temper-

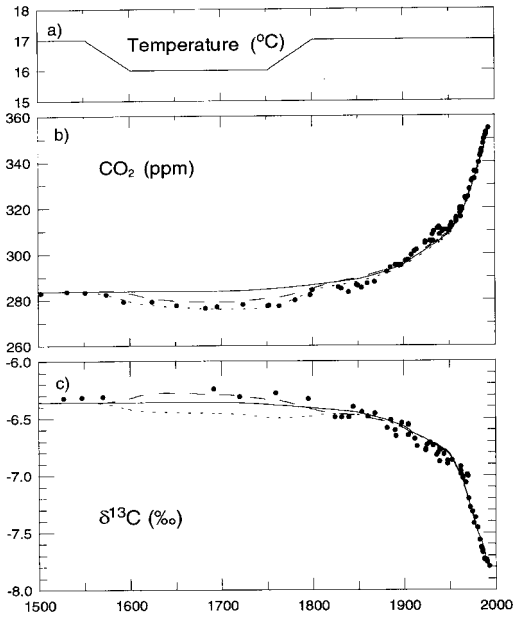

Fig. 3. (a) Hypothetical temperature record used in the LIA model calculations. (b) Modelled CO_2 and (c) modelled $\delta^{13}C$. All three cases shown in (b) and (c) include the fossil fuel burning, land-use change and CO_2 fertilisation. In addition we include temperature-dependent terrestrial exchange (long dashes) or oceanic exchange (short dashes).

ature change are very idealised, and were chosen so that modelled CO_2 would roughly match the changes in the CO_2 ice core record. It should be pointed out that although the term "Little Ice Age" is quite widely used, there is no consensus on when the LIA began or ended, and there is no evidence in temperature records of a worldwide, synchronous and prolonged cold interval (Jones and Bradley, 1992). Grove (1988) estimates that the observed temperature decrease in parts of Europe was about 1–2°C, with frequent fluctuations rather than sustained cool temperatures. We have considered a cooling of 1°C for the whole biospheric or oceanic reservoirs, but the modelled changes would also apply for a temperature change of more than 1°C over a smaller region.

The carbon cycle model is used in forward mode to calculate the change in CO_2 and $\delta^{13}C$ with the hypothetical temperature perturbation effecting either biospheric or oceanic exchange. The solid line in Fig. 3b shows modelled CO_2 due only to fossil fuel burning, land-use change and CO_2 fertilisation. As well as these sources and sinks we include temperature-dependent terrestrial exchange (long dashes) or temperature-dependent oceanic exchange (short dashes). In both cases, the decrease in temperature causes a decrease in global CO_2. Fig. 3c shows the calculated $\delta^{13}C$ for the same 3 cases. The effect of the temperature decrease on isotopic fractionation causes a decrease in $\delta^{13}C$. The temperature response of terrestrial exchange is a reduction in both NPP and soil respiration, with the reduction in soil respiration dominating. This leads to an increase in $\delta^{13}C$, which is what is measured in the ice core record.

If the temperature change had affected both terrestrial and oceanic exchange, the model would give addition of the CO_2 decrease and partial cancellation of the $\delta^{13}C$ change. However, a scenario consistent with the observed changes is that global sea surface temperatures were not significantly different during the LIA, but that major terrestrial biomes experienced significant cooling. Many of the proxy temperature records that show the cooling during this period are from northern hemisphere land sites. CH_4 from the Law Dome ice cores also shows a decrease through this period, as does the inter-polar difference of CH_4 (Etheridge et al., 1998). Harriss et al. (1993) have argued that lower land temperatures reduce the

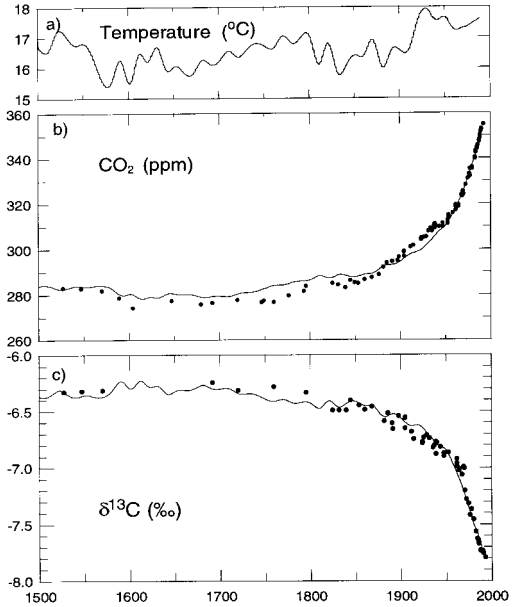

Fig. 4. (a) Northern hemisphere summer temperature anomaly from Bradley and Jones (1993). (b) CO_2 and (c) $\delta^{13}C$ calculated using a forward run with fossil fuel, land-use change, CO_2 fertilisation and temperature-dependence of biospheric exchange with the Bradley and Jones (1993) temperature record.

extent and magnitude of the CH_4 emission flux from northern hemisphere wetlands, the dominant source of pre-industrial CH_4 emissions (Chappellaz et al., 1993). Etheridge et al. (1998) therefore conclude that the lower levels of CH_4 during the LIA were linked to cooling of the northern hemisphere land surfaces, which would be supported by our calculations.

Fig. 4a shows northern hemisphere summer temperature anomalies from Bradley and Jones (1993). The CO_2 and $\delta^{13}C$ calculated by modelling the response of the terrestrial biosphere to these temperature variations (as well as fossil fuel burning, land-use change and fertilisation) is shown in Fig. 4b,c. The modelled CO_2 and $\delta^{13}C$ shows some features similar to those in the ice core record, however using only a single proxy temperature record does leave many of the features unexplained. It is likely that some regions and biomes have a stronger response to temperature changes than others, and are therefore responsible for more of the variation in global CO_2 and $\delta^{13}C$. In addition, a number of other factors are likely to

have just as much effect on global CO_2 and $\delta^{13}C$, e.g., variation in precipitation for biospheric exchange, temperature variation for oceanic fluxes or changes in ocean circulation. A number of studies have used variation in climate to calculate changes in biospheric carbon. For example, Dai and Fung (1993) used temperature and precipitation data over the period 1940–1988. There is observational evidence that variation in ocean circulation on ENSO or decadal time-scales can have an important effect on atmospheric CO_2, however much of this variation will be smoothed out in the ice core record. Recent 3-D coupled ocean/atmosphere model simulations by Sarmiento et al. (1998) and Matear and Hirst (1999) suggest that on longer time-scales, changes in ocean circulation will have only a small impact on atmospheric CO_2 for the range of climate observed over the last 1000 years. Both model studies give only about 5 GtC change in total ocean uptake up to 1990 due to the change in ocean circulation, most of which has occurred in the last few decades. Of course, current ocean models may underestimate the variability of the ocean carbon cycle, but are probably the best tool available.

Temperature records generally reflect local as well as global variations. Ice core records of long-lived trace gases from Antarctica, however, record smoothed, global signals because the diffusion and trapping processes involved in storing air in the ice lead to a smoothing of at least 10 years (Schwander et al., 1993; Trudinger et al., 1997), the trace gases are generally well mixed in the atmosphere and Antarctica is remote from terrestrial sources and sinks. Ice core records of long-lived trace gases, with this type of model calculation, have the potential not only to provide information on the carbon cycle, but also on aspects of the climate of the past.

5. Conclusions

We have described calculations with a 1-D carbon cycle model looking at natural variability and the anthropogenic perturbation in the new Law Dome CO_2 and $\delta^{13}C$ ice core record. During the LIA, the level of CO_2 was lower than mean pre-industrial levels by about 6 ppm. This decrease could have been caused by the effect of decreased temperature on either oceanic or terrestrial exchange (or both), however the observed increase in $\delta^{13}C$ during the LIA suggests terrestrial exchange as the more likely cause. Single deconvolution model calculations over the past 800 years produce generally good agreement with $\delta^{13}C$ and $\Delta^{14}C$ observations. We include the effect of the observed increase in temperature of about 0.5°C over this century, which reduces the $\delta^{13}C$ pre-industrial–modern difference by about 0.1‰, but still gives good agreement with the ice core record. Our calculated disequilibrium fluxes, and those determined by Joos and Bruno (1998), are very similar to the values from CO_2 and O_2 budget studies by Rayner et al. (1999). Natural variation in atmospheric $\Delta^{14}C$ is modelled using ^{10}Be records to reconstruct ^{14}C production rate variations. However, uncertainties in using ^{10}Be mean that at present this does not provide useful constraints on modelling other aspects of variability of CO_2 and its isotopes.

6. Acknowledgments

This work builds on long-standing collaboration with Keith Lassey (NIWA) and support from CSIRO's GASLAB and ICELAB. The authors wish to thank Martin Heimann, Pierre Friedlingstein, Fortunat Joos and Jozef Syktus for valuable comments on the manuscript, Vlad Levchenko for useful discussions and Fortunat Joos for supplying a preprint of his paper prior to publication. The CRC-SHM is funded by the Australian Government Cooperative Research Centres program.

REFERENCES

Allen, L. H., Boote, K. J., Jones, J. W., Jones, P. H., Valle, R. R., Acock, B., Rogers, H. H. and Dahlman, R. C. 1987. Response of vegetation to rising carbon dioxide: photosynthesis, biomass and seed yield of soybean. *Global Biogeochem. Cyc.* **1**, 1–14.

Andres, R. J., Marland, G., Boden, T. and Bischof, S. 1998. Carbon dioxide emissions from fossil fuel consumption and cement manufacture 1751–1991 and an estimate of their isotopic composition and latitudinal distribution. In: *The carbon cycle* (eds. Wigley, T. and

Schimel, D.). Global Change Institute, Aspen, Colorado, Cambridge University Press (in press).
Bacastow, R. B. 1981. Numerical evaluation of the evasion factor. In: *Carbon cycle modelling: SCOPE 16* (ed. Bolin, B), pp. 95–101. John Wiley and Sons, Chichester.
Bard, E., Raisbeck, G. M., Yiou, F. and Jouzel, J. 1997. Solar modulation of cosmogenic nuclide production over the last millennium: comparison between ^{14}C and ^{10}Be records. *Earth and Plan. Sci. Lett.* **150**, 453–462.
Beer, J., Siegenthaler, U., Bonani, G., Finkel, R. C., Oeschger, H., Suter, M. and Wölfli, W. 1988. Information on past solar activity and geomagnetism from ^{10}Be in the Camp Century ice core. *Nature* **331**, 675–679.
Beer, J., Joos, F., Lukasczyk, Ch., Mende, W., Rodriguez, J., Siegenthaler, U. and Stellmacher, R. 1994. ^{10}Be as an indicator of solar variability and climate. In: *The solar engine and its influence on terrestrial atmosphere and climate* (ed. Nesme-Ribes, E). NATO ASI Series, 25, 221–233.
Bradley, R. S. and Jones, P. D. 1993. "Little Ice Age" summer temperature variations: their nature and relevance to recent global warming trends. *The Holocene* **3**, 367–376.
Broecker, W. S. 1974. *Chemical oceanography*. Harcourt Brace Jovanovich, New York, 214 pp.
Broecker, W. S. and Peng, T.-H. 1974. Gas exchange rates between air and sea. *Tellus* **26**, 21–35.
Broecker, W. S., Gerard, R. and Ewing, M. 1960. Natural radiocarbon in the Atlantic ocean. *J. Geophys. Res.* **65**, 2903–2931.
Broecker, W. S., Peng, T.-H., Ostlund, G. and Stuiver, M. 1985. The distribution of bomb radiocarbon in the ocean. *J. Geophys. Res.* **90**, 6953–6970.
Bruno, M. and Joos, F. 1997. Terrestrial carbon storage during the past 200 years: A Monte Carlo analysis of CO_2 data from ice core and atmospheric measurements. *Global Biogeochem. Cycles* **11**, 111–124.
Chappellaz, J. A., Fung, I. Y. and Thompson, A. M. 1993. The atmospheric CH_4 increase since the Last Glacial Maximum (1) Source estimates. *Tellus* **45B**, 228–241.
Dai, A. and Fung, I. 1993. Can climate variability contribute to the "missing" CO_2 sink? *Global Biogeochem. Cycles* **7**, 599–609.
Duffy, P. B. and Caldeira, K. 1995. Three-dimensional model calculation of ocean uptake of bomb ^{14}C and implications for the global budget of bomb ^{14}C. *Global Biogeochem. Cycles* **9**, 373–375.
Emanuel, W. R., Killough, G. E. G. and Olson, J. S. 1981. Modelling the circulation of carbon in the world's terrestrial ecosystems. In: *Carbon cycle modelling, SCOPE 16* (ed. Bolin, B.), pp. 335–353. John Wiley and Sons, Chichester.
Enting, I. G. 1982. *Nuclear weapons data for use in carbon cycle modelling*. Division of Atmospheric Physics Technical Paper No. 44, CSIRO (Australia).
Enting, I. G. 1992. The incompatibility of ice-core CO_2 data with reconstructions of biotic CO_2 sources (II). The influence of CO_2-fertilised growth. *Tellus* **44B**, 23–32.
Enting, I. G. and Lassey, K. R. 1993. *Projections of future CO_2*. CSIRO Division of Atmospheric Research Technical Paper No. 27, CSIRO (Australia).
Enting, I. G. and Pearman, G. I. 1982. *Description of a one-dimensional global carbon cycle model*. Division of Atmospheric Physics Technical Paper No. 42, CSIRO (Australia).
Enting, I. G. and Pearman, G. I. 1987. Description of a one-dimensional carbon cycle model calibrated using techniques of constrained inversion. *Tellus* **39B**, 459–476.
Enting, I. G., Wigley, T. M. L. and Heimann, M. 1994. *Future emissions and concentrations of carbon dioxide: key ocean/atmosphere/land analyses*. CSIRO Division of Atmospheric Research Technical Paper No. 31, CSIRO (Australia).
Enting, I. G., Trudinger, C. M. and Francey, R. J. 1995. A synthesis inversion of the concentration and $\delta^{13}C$ of atmospheric CO_2. *Tellus* **47B**, 35–52.
Etheridge, D. M., Steele, L. P., Langenfelds, R. L., Francey, R. J., Barnola, J.-M. and Morgan, V. I. 1996. Natural and anthropogenic changes in atmospheric CO_2 over the last 1000 years from air in Antarctic ice and firn. *J. Geophys. Res.* **101D**, 4115–4128.
Etheridge, D. M., Steele, L. P., Francey, R. J. and Langenfelds, R. 1998. Atmospheric methane between 1000 AD and present: evidence for anthropogenic emissions and climatic variability. *J. Geophys. Res.* **103**, 15979.
Francey, R. J., Tans, P. P., Allison, C. E., Enting, I. G., White, J. W. C. and Troller, M. 1995. Changes in oceanic and terrestrial carbon uptake since 1982. *Nature* **373**, 326–330.
Francey, R. J., Allison, C. E., Etheridge, D. M., Trudinger, C. M., Enting, I. G., Leuenberger, M., Langenfelds, R. L., Michel, E. and Steele, L. P. 1999. A 1000-year high precision record of $\delta^{13}C$ in atmospheric CO_2. *Tellus* **51B**, 170–193.
Friedli, H., Lötscher, H., Oeschger, H., Siegenthaler, U. and Stauffer, B. 1986. Ice core record of the $^{13}C/^{12}C$ ratio of atmospheric CO_2 in the past two centuries. *Nature* **324**, 237–238.
Grace, J., Malhi, Y., Lloyd, J., McIntyre, J., Miranda, A. C., Meir, P. and Miranda, H. S. 1996. The use of eddy covariance to infer the net carbon dioxide uptake of Brazilian rain forest. *Glob. Change Biol.* **2**, 209–217.
Grove, J. M. 1988. *The Little Ice Age*. Methuen, New York, 498 pp.
Harriss, R., Bartlett, K., Frolking, S. and Crill, P. 1993. Methane emissions from northern high-latitude wetlands. In: *Biogeochemistry of global change: radiatively active trace gases* (ed. Oremland, R. S.), pp. 449–486. Chapman and Hall, New York.
Harvey, L. D. D. 1989. Effect of model structure on the response of terrestrial biosphere models to CO_2 and temperature increases. *Global Biogeochem. Cycles* **3**, 137–153.

Heimann, M. and Keeling, C. D. 1989. A three-dimensional model of atmospheric CO_2 transport based on observed winds: 2. Model description and simulated tracer experiments. In: *Aspects of climate variability in the Pacific and Western Americas* (ed. Peterson, D. H). Geophys. Monogr. Ser., vol. **55**, pp. 237–275.

Heimann, M. and Maier-Reimer, E. 1996. On the relations between the oceanic uptake of CO_2 and its carbon isotopes. *Global Biogeochem. Cycles* **10**, 89–110.

Hesshaimer, V., Heimann, M. and Levin, I. 1994. Radiocarbon evidence for a smaller oceanic carbon dioxide sink than previously believed. *Nature* **370**, 201–203.

Hodgeman, C. D. 1958. *Handbook of chemistry and physics*. Chemical Rubber Pub. Co. (Cleveland).

Houghton, R. A. 1995. Effects of land-use change, surface temperature and CO_2 concentration on terrestrial stores of carbon. In: *Biotic feedbacks in the global climatic system: will the warming feed the warming?* (eds. Woodwell, G. M. and Mackenzie, F. T.), pp. 333–350. Oxford University Press, Oxford.

Houtermans, J. C. 1971. *Geophysical interpretations of bristlecone pine radiocarbon measurements using a method of fourier analysis of unequally spaced data*. Thesis, University of Bern, Bern.

Jain, A. K., Kheshgi, H. S. and Wuebbles, D. J. 1996. A globally aggregated reconstruction of cycles of carbon and its isotopes. *Tellus* **48B**, 583–600.

Jain, A. K., Kheshgi, H. S. and Wuebbles, D. J. 1997. Is there an imbalance in the global budget of bomb-produced radiocarbon? *J. Geophys. Res.* **102D**, 1327–1333.

Jones, P. D. and Bradley, R. S. 1992. Climatic variations over the last 500 years. In: *Climate since AD 1500* (eds. Bradley, R. S. and Jones, P. D.), pp. 649–665. Routledge, New York.

Jones, P. D. and Briffa, K. R. 1992. Global surface air temperature variations during the twentieth century. Part 1. Spatial, temporal and seasonal details. *The Holocene* **2**, 165–179.

Joos, F. 1994. Imbalance in the budget. *Nature* **370**, 181–182.

Joos, F. and Bruno, M. 1998. Decadal variability of the terrestrial and oceanic carbon sinks and the budgets of the carbon isotopes ^{13}C and ^{14}C. *Global Biogeochem. Cycles* **12**, 277–295.

Keeling, C. D., Bacastow, R. B., Carter, A. F., Piper, S. C., Whorf, T. P., Heimann, M., Mook, W. G. and Roeloffzen, H. 1989. A three-dimensional model of atmospheric CO_2 transport based on observed winds (1). Analysis of observational data. In: *Aspects of climate variability in the Pacific and Western Americas* (ed. Peterson, D. H). Geophys. Monogr. Ser., vol. **55**, 165–236.

Keeling, C. D. 1997. Global historical CO_2 emissions. In: *Trends: a compendium of data on global change*. Carbon Dioxide Information Analysis Center, Oak Ridge National Laboratory, Oak Ridge, Tenn., USA.

Lassey, K. R., Enting, I. G. and Trudinger, C. M. 1996. The earth's radiocarbon budget: A consistent model of the global carbon and radiocarbon cycles. *Tellus* **48B**, 487–501.

Levin, I., Kromer, B., Schoch-Fischer, H., Bruns, M., Munnich, M., Berdau, D., Vogel, J. C. and Munnich, K. O. 1985. 25 years of tropospheric ^{14}C observations in central Europe. *Radiocarbon* **27**, 1–19.

Manning, M. R. and Melhuish, W. H. 1994. Atmospheric $\Delta^{14}C$ record from Wellington. In: *Trends '93: A compendium of data on global change*, pp. 193–202. Carbon Dioxide Information Analysis Center, Oak Ridge National Laboratory, Oak Ridge, Tenn., USA.

Marland, G., and Boden, T. A. 1997. Global, regional, and national CO_2 emissions. In: *Trends: A compendium of data on global change*. Carbon Dioxide Information Analysis Center, Oak Ridge National Laboratory, Oak Ridge, Tenn., USA.

Martin, J. H., Knauer, G. A., Karl, D. M. and Broenkow, W. W. 1987. VERTEX: carbon cycling in the northeast Pacific. *Deep Sea Res.* **34**, 267–285.

Matear, R. and Hirst, T. 1999. Climate change feedback on the future oceanic CO_2 uptake. *Tellus*, in press.

Mook, W. G., Bommerson, J. C. and Staverman, W. H. 1974. Carbon isotope fractionation between dissolved bicarbonate and gaseous carbon dioxide. *Earth and Planetary Science Letters* **22**, 169–176.

Oeschger, H., Siegenthaler, U., Schotterer, U. and Guglemann, A. 1975. A box-diffusion model to study the carbon dioxide exchange in nature. *Tellus* **27**, 168–192.

Raisbeck, G. M., Yiou, F., Jouzel, J. and Petit, J. R. 1990. ^{10}Be and δ^2H in polar ice cores as a probe of the solar variability's influence on climate. *Phil. Trans. R. Soc. Lond. A* **330**, 463–470.

Rayner, P. J., Enting, I. G., Francey, R. J. and Langenfelds, R. 1999. Reconstructing the recent carbon cycle from atmospheric CO_2, $\delta^{13}C$ and O_2/N_2 observations. *Tellus* **51B**, 210–212.

Sarmiento, J. L, Hughes, T. M. C., Stouffer, R. J. and Manabe, S. 1998. Simulated response of the ocean carbon cycle to anthropogenic climate warming. *Nature* **393**, 245–249.

Schwander, J., Barnola, J.-M., Andrie, C., Leuenberger, M., Ludin, A., Raynaud, D. and Stauffer, B. 1993. The age of the air in the firn and the ice at Summit, Greenland. *J. Geophys. Res.* **98**, 2831–2838.

Siegenthaler, U. and Joos, F. 1992. Use of a simple model for studying oceanic tracer distributions and the global carbon cycle. *Tellus* **44B**, 186–207.

Siegenthaler, U. and Oeschger, H. 1987. Biospheric CO_2 emissions during the past 200 years reconstructed by deconvolution of ice core data. *Tellus* **39B**, 140–154.

Stuiver, M. and Becker, B. 1993. High-precision decadal calibration of the radiocarbon time scale, AD 1950–6000 BC. *Radiocarbon* **35**, 35–65.

Stuiver, M. and Quay, P. D. 1980. Changes in atmospheric carbon-14 attributed to a variable sun. *Science* **207**, 11–19.

Stuiver, M. and Quay, P. D. 1981. Atmospheric ^{14}C changes resulting from fossil fuel CO_2 release and cosmic ray flux variability. *Earth and Planetary Science Letters* **53**, 349–362.

Suess, H. E. 1955. Radiocarbon concentration in modern wood. *Science* **122**, 415–417.

Tans, P. 1981. A compilation of bomb ^{14}C data for use in global carbon model calculations. In: *Carbon cycle modelling, SCOPE 16* (ed. Bolin, B.), pp. 131–157. John Wiley and Sons, Chichester.

Tans, P. P., Berry, J. A. and Keeling, R. F. 1993. Oceanic $^{13}C/^{12}C$ observations: a new window on ocean CO_2 uptake. *Global Biogeochem. Cycles* **7**, 353–368.

Telegadas, K. 1971. *The seasonal atmospheric distribution and inventories of excess carbon-14 from March 1955 to July 1969*. In: Health and Safety Lab. Rep. 243, pp. 2–87. US At. Energy Comm., Washington, DC, USA.

Trudinger, C. M., Enting, I. G., Etheridge, D. M., Francey, R. J., Levchenko, V. A., Steele, L. P., Raynaud, D. and Arnaud, L. 1997. Modelling air movement and bubble trapping in firn. *J. Geophys. Res.* **102D**, 6747–6763.

Zhang, J., Quay, P. D. and Wilbur, D. O. 1995. Carbon isotope fractionation during gas–water exchange and dissolution of CO_2. *Geochim. Cosmochim. Acta* 59, 107–114.